

# Heteroepitaxial BiFeO<sub>3</sub> Films Fabricated on MgO(001) and Sr<sub>0.61</sub>Ba<sub>0.39</sub>Nb<sub>2</sub>O<sub>6</sub>/MgO(001)



D. V. Stryukov, A. V. Pavlenko, L. I. Kiseleva, and G. N. Tolmachev

**Abstract** BiFeO<sub>3</sub>/MgO(001) and BiFeO<sub>3</sub>/Sr<sub>0.61</sub>Ba<sub>0.39</sub>Nb<sub>2</sub>O<sub>6</sub>/MgO(001) heterostructures were deposited by a one-stage technique of RF-cathode sputtering of a stoichiometric composition ceramic target in an oxygen atmosphere. The films were studied by X-ray diffraction and scanning electron microscopy at room temperature. It is shown that the heterostructures have high crystal perfection and a low number of structural defects. It was found that the bismuth ferrite unit cell has monoclinic symmetry in the BiFeO<sub>3</sub>/MgO(001) heterostructure. There is only a slight unit cell strain in both heterostructures. The presence of the Sr<sub>0.61</sub>Ba<sub>0.39</sub>Nb<sub>2</sub>O<sub>6</sub> between BiFeO<sub>3</sub> and MgO does not break the parallel of their crystallographic axes.

**Keywords** Thin film · Heterostructure · X-ray diffraction · Bismuth ferrite · Strontium-barium niobate

## 1 Introduction

In modern terminology, materials in which two or more types of orderings coexist simultaneously (ferroelectric, magnetic, and ferroelastic) are commonly termed as multiferroics. Interest in them continues to this day due to the wide range of their possible applications in multifunctional devices [1]. The greatest attention is drawn to the relationship between different order parameters, which can lead to new physical effects, such as, for example, the control of magnetic properties by electric field or vice versa. One of the important criteria for the use of multiferroics is the room temperature ordering [2]. However, there are very few single-phase multiferroics that satisfy this condition, among which the most famous is bismuth ferrite BiFeO<sub>3</sub> (BFO), a multiferroic with a perovskite structure, in which ferroelectric and antiferromagnetic orderings are realized. Bulk BFO has a rhombohedral unit cell with the R3c space group. The temperatures of both phase transitions are significantly higher than

---

D. V. Stryukov (✉) · A. V. Pavlenko · L. I. Kiseleva · G. N. Tolmachev  
Federal Research Centre the Southern Scientific Centre of the Russian Academy of Sciences,  
Rostov-on-Don 344006, Russia  
e-mail: [strdl@mail.ru](mailto:strdl@mail.ru)

room temperature ( $T_C \sim 1100$  K;  $T_N \sim 640$  K) [1–5], and the remanent polarization along the [111] polar direction sufficiently high for ferroelectric materials ( $P_r \sim 100 \mu\text{C}/\text{cm}^2$ ) [3, 4]. All the above makes bismuth ferrite a promising candidate for use in high-density ferroelectric memory devices. Moreover, many other effects have been found in BFO, such as magnetoelectric, magnetodielectric and photovoltaic effects, and birefringence.

To date, BFO thin films have already been fabricated by various deposition technologies: pulsed laser deposition [6, 7], sol–gel [8], magnetron sputtering [9]. Due to the presence of a large number of impurity phases arising in the process of BFO synthesis, additional annealing after synthesis [7, 8] or preliminary deposition of sublayers [6, 9] are often used in the technological cycle of fabricating heterostructures based on it. The use of an additional layer based on functional materials can not only prevent the appearance of impurities but it is also one of the most promising steps towards the creation of new microelectronic devices, where interactions between different orderings of functional layers can occur. As an additional layer, the strontium-barium niobate  $\text{Sr}_x\text{Ba}_{1-x}\text{Nb}_2\text{O}_6$  was chosen.  $\text{Sr}_x\text{Ba}_{1-x}\text{Nb}_2\text{O}_6$  solid solution is a uniaxial ferroelectric relaxor with the structure of unfilled tetragonal potassium-tungsten bronze. Interest in them is due to the high electro-optical and pyroelectric coefficients [10], that can be used in MEMS, electro-optical elements, and pyroelectric sensors.

## 2 Problem Formulation

It has been studied by X-ray diffraction analysis and SEM microscopy the structure of BFO thin films grown with and without a  $\text{Sr}_{0.61}\text{Ba}_{0.39}\text{Nb}_2\text{O}_6$  sublayer on MgO (001) substrate by a one-stage gas-discharge RF-cathode sputtering in an oxygen atmosphere.

### 2.1 Objects and Methods

The deposition of  $\text{BiFeO}_3$  (BFO) and  $\text{Sr}_{0.61}\text{Ba}_{0.39}\text{Nb}_2\text{O}_6$  (SBN) thin films was carried out by RF-cathode sputtering technique on a “Plasma 50 SE” system (Center for Collective Use of the SSC RAS) in an oxygen atmosphere using the intermittent deposition technology. As a substrate MgO(001) monocrystalline plates of 0.5 mm thick were used, the initial temperature of the substrate was 400 °C and the working gas pressure was 0.5–0.6 Torr.

The structural perfection of the films, the unit cell parameters and the orientation relationships between film and substrate were performed by X-ray diffraction on a DRON-4–07 diffractometer ( $\text{CuK}\alpha$ -radiation).

Microscopic studies of the heterostructures were carried out on an FE-SEM Zeiss SUPRA 25 scanning electron microscope.

## 2.2 Experimental Results and Discussion

The X-ray diffraction studies of the BFO/MgO(001) and BFO/SBN/MgO(001) heterostructures do not show any traces of impurity phases and on the diffraction patterns, only reflections from the heterostructure layers and the substrate were registered (Fig. 1). It should be noted that during the searching for optimal conditions for the heterostructure synthesis of both SBN and BFO, lines of impurity phases were founded, but due to the weakness of reflections, it was unable to establish a type of impurities.

The BFO film grows oriented relative to the substrate axes in both cases. The  $\varphi$ -scans (Fig. 2) of the (113) BFO thin film reflection confirm epitaxial growth, with the orientation of all crystallographic axes of the BFO parallel to the axes of the substrate in both heterostructures. The SBN layer is also fabricated epitaxially. Moreover, the parallel orientation of BFO is observed even in the presence of an SBN layer, which, similarly to [11], have two types of orientation domains with an in-plane rotation of the axes by  $+18.4^\circ$  and  $-18.4^\circ$ .

At the precision  $\theta$ - $2\theta$ -scanning of (00l) reflections (Fig. 3) of the two-layer BFO/SBN/MgO(001) heterostructure, a splitting of the reflections corresponding to separate scattering by each layer is observed. From the analysis of the angular positions of the (00l) reflections, taking into account the  $K_{\alpha 1}$  and  $K_{\alpha 2}$  components in the obtained X-ray diffraction patterns, the out-of-plane unit cell parameters are  $c_{\text{BFO}} = 3.964 \pm 0.001 \text{ \AA}$  for BFO/MgO(001) and  $c_{\text{BFO}} = 3.960 \pm 0.001 \text{ \AA}$ ,  $c_{\text{SBN}} = 3.972 \pm 0.001 \text{ \AA}$  for BFO/SBN/MgO(001). The addition of the SBN layer results in a slight decrease in the BFO unit cell parameter, corresponding to  $-0.1\%$  additional unit cell strain.

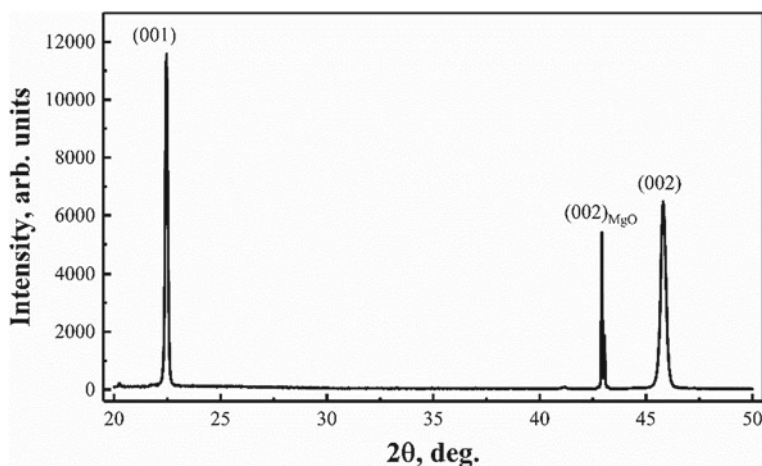


**Fig. 1**  $\theta$ - $2\theta$  diffraction pattern of BFO/MgO(001)

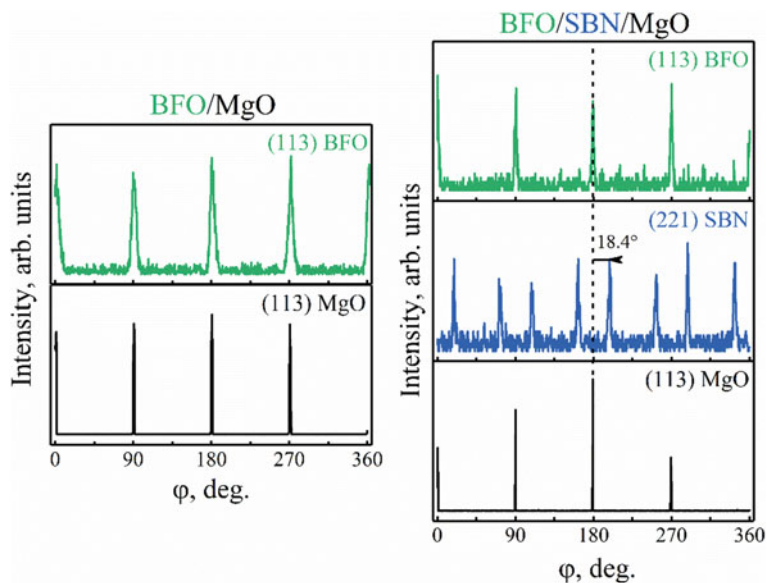


**Fig. 2**  $\phi$ -scans of (113) BFO, (221) SBN and (113) MgO reflections for BFO/MgO(001) and BFO/SBN/MgO(001) heterostructures

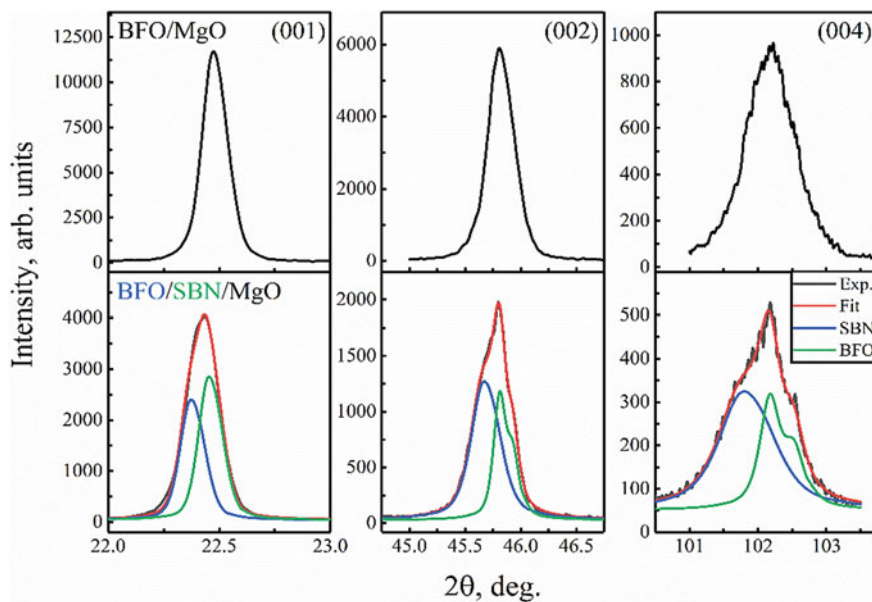
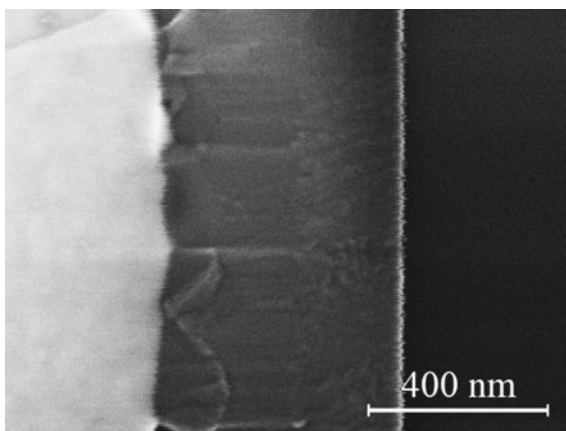


**Fig. 3** Precision  $\theta$ - $2\theta$ -scanning of (001) reflections for BFO/MgO(001) (top) and BFO/SBN/MgO(001) (bottom) heterostructures

**Fig. 4** SEM image of mechanical cross-cut of BFO/SBN/MgO(001) heterostructure



To determine the in-plane unit cell parameters a series of (113) and (103) reflections of the BFO/MgO(001) heterostructure in an asymmetric geometry were obtained. Within the accuracy of the obtained X-ray diffraction data, for BFO the most probable is the following monoclinic unit cell  $a = b = c = 3.964$  nm,  $\alpha = \beta = 89.75^\circ$ ,  $\gamma = 90^\circ$ . Comparing the obtained parameters with the parameters of bulk BFO ( $a = 3.965$  Å;  $\alpha = 89.45^\circ$ ), it can be seen that the unit cell strain is insignificant.

The films have high crystal perfection and a low number of structural defects, which appear in narrow reflections on the  $\theta$ - $2\theta$  and  $\varphi$  scans. The misorientations of the crystallographic axes are insignificant and do not exceed  $0.7^\circ$ . The high crystalline perfection, homogeneity and absence of impurities were also approved by SEM cross-cut studies of BFO/SBN/MgO(001) heterostructure (Fig. 4). Each layer of the two-layer heterostructure differs in texture and color, which is due to both different compositions and different electrical properties, while the interface is fairly uniform. Pores, cavities, inclusions of impurity phases have not been found.

### 3 Conclusion

BFO epitaxial films on MgO (001) substrates with and without an SBN epitaxial layer were obtained by the RF-cathodic sputtering technique. By deposition a sufficiently thick film, it was possible to achieve almost complete relaxation of the unit cell strain. It was found that the deposition of an intermediate SBN layer does not lead to a significant change in the unit cell parameters. It was shown that the presence of two types of orientational domains in the SBN layer ( $\pm 18.4^\circ$ ) does not lead to a rotation of the BFO unit cell.

**Acknowledgements** This study was performed within a government contract for the Southern Scientific Center of the Russian Academy of Sciences (project no. 0120-1354-247) and supported by grant No. MK-678.2020.2 of the President of the Russian Federation.

## References

1. J.F. Scott, *J. Mater. Chem.* **22**, 4567 (2012)
2. N.A. Hill, *J. Phys. Chem. B.* **104**(29), 6694 (2000)
3. R.R. Das, D.M. Kim, S.H. Baek, C.B. Eom, F. Zavaliche, S.Y. Yang, R. Ramesh, Y.B. Chen, X.Q. Pan, X. Ke, M.S. Rzchowski, S.K. Streiffer, *Appl. Phys. Lett.* **88**, 242904 (2006)
4. J. Li, J. Wang, M. Wuttig, R. Ramesh, N. Wang, B. Ruetter, A.P. Pyatakov, A.K. Zvezdin, D. Viehland, *Appl. Phys. Lett.* **84**, 5261 (2004)
5. J. Wang, J.B. Neaton, H. Zheng, V. Nagarajan, S.B. Ogale, B. Liu, D. Viehland, V. Vaithyanathan, D.G. Schlom, U.V. Waghmare, N.A. Spaldin, K.M. Rabe, M. Wuttig, R. Ramesh, *Science* **299**, 1719 (2003)
6. C.-Y. Kuo, Z. Hu, J.C. Yang, S.-C. Liao, Y.L. Huang, R.K. Vasudevan, M.B. Okatan, S. Jesse, S.V. Kalinin, L. Li, H.J. Liu, C.-H. Lai, T.W. Pi, S. Agrestini, K. Chen, P. Ohresser, A. Tanaka, L.H. Tjeng, Y.H. Chu, *Nat. Commun.* **7**, 12712 (2016)
7. F. Aziz, P. Pandey, M. Chandra, A. Khare, D.S. Rana, K.R. Mavani, *J. Magn. Magn. Mater.* **356**, 98 (2014)
8. M. Tyagi, R. Chatterjee, P. Sharma, *J. Mater. Sci.: Mater. Electron.* **26**, 1987 (2015)
9. Y.-H. Lee, C.-C. Lee, Z.-X. Liu, C.-S. Liang, J.-M. Wu, *Electrochem. Solid-State Lett.* **9**(5), F38 (2006)
10. Yu S Kuz'minov, *Ferroelectric Crystals for Control of Laser Radiation* (Nauka, Moscow, 1982), p. 400 (In Russian)
11. A.V. Pavlenko, L.I. Ivleva, D.V. Stryukov, A.P. Kovtun, A.S. Anokhin, P.A. Lykov, *Phys. Solid State* **61**, 244 (2019)